Journal of Power Sources 195 (2010) 2541–2548

Contents lists available at ScienceDirect

Journal of Power Sources

journal homepage: www.elsevier.com/locate/jpowsour

Organic–inorganic crosslinked and hybrid membranes derived from sulfonated poly(arylene ether sulfone)/silica via sol–gel process

Shaoguang Feng[a], Yuming Shang[a], Yingzi Wang[a], Xiaofeng Xie[a,*], V.K. Mathur[b], Jingming Xu[a]

[a] Institute of Nuclear and New Energy Technology, Tsinghua University, Beijing 100084, PR China
[b] Department of Chemical Engineering, University of New Hampshire, NH 03824, USA

ARTICLE INFO

Article history:
Received 5 September 2009
Received in revised form 6 November 2009
Accepted 9 November 2009
Available online 24 November 2009

Keywords:
Direct methanol fuel cell
Proton conductive membrane
Covalently crosslinked
Sulfonated poly(arylene ether sulfone)
Hybrid

ABSTRACT

A series of covalently crosslinkable organic–inorganic hybrid membranes have been prepared from sulfonated poly(arylene ether sulfone) (SPAES) with pendant propenyl moiety and various amounts of vinyl substituted silica via sol–gel process which are then thermally crosslinked in the presence of benzoyl peroxide (BPO) initiator. The obtained membranes are characterized in terms of oxidative stability, thermal property, ion exchange capacity (IEC), water uptake, swelling ratio in methanol aqueous solution, proton conductivity, and methanol permeability coefficient. The results indicate that the oxidative stability and thermal stability of the hybrid membranes are improved. Moreover, introduction of silica reduces the water uptake and methanol swelling of membranes. The swelling ratio of membranes in 2 mol L^{-1} methanol aqueous solution at 80 °C slowly decreases from 26 to 19% with the increase of SiO_2 content from 0 to 12 wt.%. Furthermore, with the increase in silica content, the methanol permeability coefficient of the hybrid membranes decreases at first and then increases. When the silica content reaches 8 wt.%, the methanol permeability coefficient is at the minimum of 6.02×10^{-7} cm^2 s^{-1}, a 2.64-fold decrease compared with that of the pristine SPAES membrane. Moreover, the proton conductivity is found to be at about 95% of that of pristine polymer at that silica content.

1. Introduction

Direct methanol fuel cells (DMFCs) are attractive as promising power source for portable applications due to their several advantages: no fuel processing unit, low temperature and pressure operation, high energy efficiency and low emission, compact cell design, etc. [1–3]. Proton exchange membrane (PEM) is one of the key components of a DMFC, which serves as an electrolyte for transporting protons from anode to cathode without allowing fuel crossover. Currently, the widely used proton exchange membranes are perfluorosulfonic acid membranes, such as Nafion manufactured by DuPont. However, Nafion has some shortcomings which limit its utility and performance, such as the high cost, low working temperature and high methanol permeability [4–8]. Therefore, one of the challenges in DMFC research is the development of novel PEM by increasing proton conductivity and reducing methanol permeability to improve the cell performance [9]. Recently, several non-fluorinated membranes such as sulfonated poly(arylene ether), sulfonated polyimide (SPI) and acid-doped polybenzimidazole (PBI), etc. have been investigated as potentially PEM materials [10–12]. Among the numerous alternative polymers, sulfonated poly(arylene ether)s such as sulfonated poly(arylene ether ketone)s, sulfonated poly(arylene ether sulfone)s [13–15] are good candidates due to their superior acidic and high glass transition temperatures and excellent mechanical strengths. Compared with perfluorinated sulfonic acid membranes, sulfonated poly(arylene ether) is reported to possess a smaller characteristic separation length and wider distribution of the proton-conducting channels with more dead-end channels and a larger internal interface between the hydrophobic and hydrophilic domains, which will affect the permeability of methanol [16]. Generally, these sulfonated hydrocarbon polymer membranes require a high sulfonation level to achieve sufficient proton conductivity. Unfortunately, such a high sulfonation level usually makes them excessively swell and even soluble in methanol/water solution, leading to a deterioration in mechanical properties and high methanol permeation [17]. Therefore, much effort has been expended in modification the membranes to improve their dimensional stability and reduce the methanol crossover at sufficient sulfonation level [18–21].

Crosslinking could be a reasonable method for improving the dimensional stability and avoiding the irreversible swelling of membranes [21,22], Zhong et al. [20] synthesized crosslinkable sulfonated poly(ether ether ketone)s containing unsaturated propenyl group which could be crosslinked using usual thermal activated

* Corresponding author. Tel.: +86 10 6278 4827; fax: +86 10 6278 4827.
E-mail addresses: ymshang@mail.tsinghua.edu.cn (Y. Shang), xiexf@mail.tsinghua.edu.cn (X. Xie).

0378-7753/$ – see front matter © 2009 Elsevier B.V. All rights reserved.
doi:10.1016/j.jpowsour.2009.11.034

radical crosslinking agent. The crosslinked membranes exhibit excellent dimensional stability and little loss in proton conductivity.

Furthermore, organic–inorganic hybrid membranes have attracted much attention as PEM for fuel cells because such hybrids may provide controllable chemical and physical properties by combining the effects of organic polymers and inorganic compounds [23–25]. The organic component may provide mechanical strength and proton conductivity, whereas the inorganic phase can reduce methanol crossover and improve both thermal and chemical stabilities [26]. Several studies have showed that the presence of inorganic particles in the organic polymer matrix can reduce the methanol permeability of the hybrids due to the dispersed particles acting as methanol barriers [9,27,28]. Chuang et al. [27] prepared polybenzimidazole (PBI)/silica nanocomposite membranes via sol–gel process from PBI copolymer with a silica precursor, tetraethoxysilane (TEOS), and a bonding agent. The introduction of the bonding agent resulted in the reinforced interfacial interaction between PBI chains and silica nanoparticles. The methanol permeability of the PBI/10 wt.% silica nanocomposite membrane decreased 58% with respect to the pure PBI membrane.

The objective of this study was to prepare organic–inorganic hybrid membranes in combination with crosslinked structure with a lot of merits mentioned above and to determine the effects of the integrated microstructure on PEM performances. The silica particles within the membranes were used to blocking excessive methanol crossover and crosslinking networks were responsible to improve their dimensional stability. Sulfonated poly(arylene ether sulfone) (SPAES) with pendant propenyl moiety and silica hybrid PEM were prepared by sol–gel method using tetraethoxysilane (TEOS) and triethoxyvinylsilane (TEOVS) as an inorganic precursor under acidic condition. Firstly, SPAES was synthesized from 4,4′-biphenol (BP), 3,3′-diallyl-4,4′-dihydroxybiphenyl (ABP), 4,4′-dichlorodiphenylsulfone (DCDPS) and 3,3′-disulfonated-4,4′-dichlorodiphenyl sulfone (SDCDPS), as shown in Scheme 1. The synthesized SPAES was mixed with sol of TEOS and TEOVS to form the vinyl substituted silica/SPAES composites which were further subjected to thermally treatment in the presence of benzoyl peroxide (BPO) to initiate the double bond reaction for the formation of covalently crosslinked networks. The crosslinkage conjoined not only polymer chains with polymer chains, but also polymer chains with silica moieties. The covalent bonding between polymer chains and silicas reinforced the interfacial interaction between organic and inorganic phases. The molecular structure and morphology of the prepared SPAES/silica hybrid membranes were characterized by FT-IR and scanning electron microscopy (SEM), respectively. The water uptake, swelling ratio, proton conductivity and methanol permeability of the prepared hybrid membranes were studied and correlated with the molecular structure.

2. Experimental

2.1. Materials

4,4′-Dichlorodiphenylsulfone (DCDPS) and 4,4′-biphenol (BP) were purchased from Weisi Chemical Company and dried under vacuum at 60 °C for 24 h prior to use. 3,3′-Diallyl-4, 4′-dihydroxybiphenyl (ABP) was prepared as outlined elsewhere [29], and dried under vacuum at 50 °C for 24 h before use. The 3,3′-disulfonated 4,4′-dichlorodiphenyl sulfone (SDCDPS) was synthesized as outlined in Ref. [30], and dried under vacuum at 160 °C for 24 h before use. Potassium carbonate (purchased from Beijing Chemical Reagent Co.) was dried under vacuum at 140 °C for 24 h before use. Benzoyl peroxide (BPO) (AR) was provided by Beijing Chemical Reagent Co. and was recrystallized twice from the mixture of $CHCl_3$/CH_3OH. N,N′-dimethylacetamide (DMAc), N-methyl-2-pyrrolidinone (NMP), triethoxyvinylsilane (TEOVS, 97%) and tetraethoxysilane (TEOS, 99%) were purchased from Beijing Chemical Reagent Co. and used without further purification. Other chemicals and solvents were obtained from commercial sources and used as received.

2.2. Synthesis of SPAES with pendant propenyl moiety

The synthetic procedure to prepare disulfonated copolymers with 40 mol.% disulfonation and 10 mol.% ABP unit is shown in Scheme 1. Firstly, 1.6759 g (9 mmol) BP, 0.2664 g (1 mmol) ABP, 1.7230 g (6 mmol) DCDPS, and 1.9650 g (4 mmol) SDCDPS were added to a three-necked flask equipped with a mechanical stirrer, nitrogen inlet, Dean Stark trap and a condenser. Next, 1.5894 g (11.5 mmol) potassium carbonate and 28 ml NMP were introduced. Toluene (14 ml) was used as an azeotropic agent. The reaction mixture was heated under reflux at 155 °C for 4 h to dehydrate the system. The mixture was further reacted for 24 h during which the solution became very viscous after the temperature was increased slowly to 175 °C by controlled removal of the toluene. The solution obtained was then cooled to room temperature and diluted with DMAc, followed by filtration to remove most of the salts and iso-

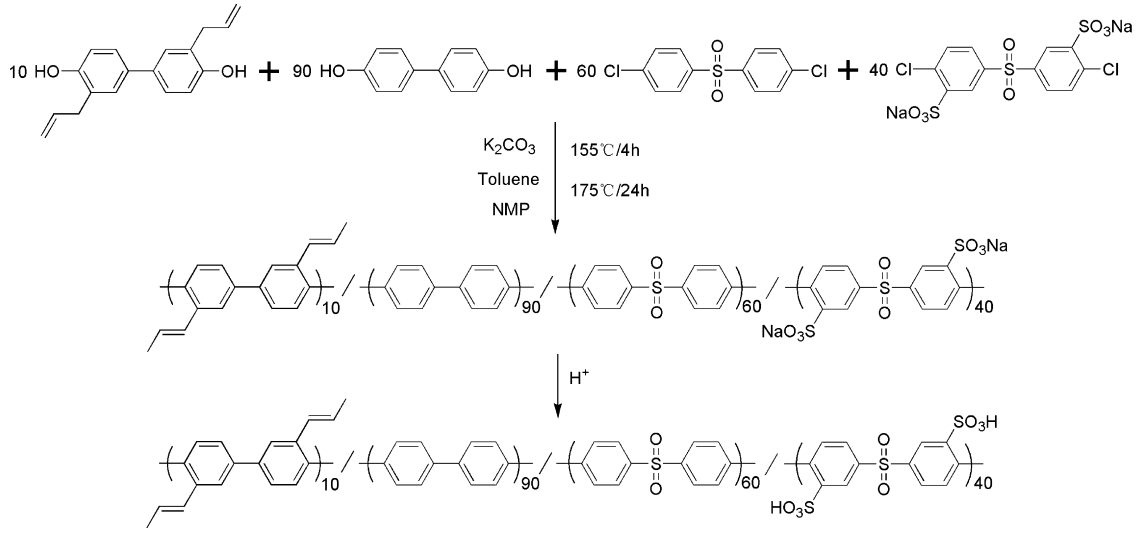

Scheme 1. Synthesis of SPAES pendant propenyl moiety.

lated as swollen strings by the addition into stirred deionized water. The precipitated polymer was washed several times with deionized water to fully remove salts and then dried at 120 °C for 24 h prior to use. The copolymer synthesized was designated as ANa10 (salt form) or AH10 (acid form), where 10 represents the ABP content as 10 mol.%.

2.3. Membrane preparation

Organic–inorganic hybrids using the ANa10 and sol–gel derived silica were prepared by dissolving ANa10 in DMAc followed by the addition of a mixture of TEOS and TEOVS (TEOS/TEVOS = 5/1, mol/mol) to the solution. The TEOS and TEOVS mixture was prepared by mixing H_2O/(TEOS + TEVOS)/HCl in a mole ratio of 4/1/0.1, which was stirred at room temperature for 1 h. Then, the ANa10/silica solutions were mixed together along with BPO for each composition, and the mixture was stirred for 6 h at 30 °C under N_2 gas. The mixed solution was then poured onto a clean glass plate and dried at 40 °C for 48 h until most of solvent was removed. The dried membranes were peeled off away from the glass plate, and then heated in an oven at 180 °C for 1.5 h to induce reaction. The hybrid membranes were converted to the required acid form by immersion in 0.5 mol L^{-1} sulfuric acid solution at 100 °C for 2 h, followed by treatment with boiling deionized water for 2 h. Thus prepared membranes with the thickness of about 60 μm were designated as AH10/SiO_2-*X*, where *X* refers to weight percentage of silica relative to AH10 copolymer.

2.4. Characterization

FT-IR spectra were obtained with a Shimadzu-FTIR-8400 Fourier transform infrared spectrophotometer.

Scanning electron microscopy (SEM) measurements were performed on a HITACHI S-5500 microscope with energy dispersive X-ray spectrometry (EDX). The membrane samples were fractured by immersing in liquid nitrogen and coated with carbon under vacuum. The cross-sectional morphology of membranes was observed by SEM.

The oxidation stability of the membranes was evaluated by immersing the samples in a Fenton's reagent (3% H_2O_2 containing 2 ppm $FeSO_4$) at 80 °C. The stability was evaluated by recording the time when membranes began to break into pieces.

Thermo-gravimetric analysis (TGA) was recorded on a PerkinElmer 7 series thermal analysis system at a heating rate of 10 °C min^{-1} under N_2 atmosphere. Before testing, all the membranes were preheated to 150 °C and kept at this temperature for 30 min to remove any residual moisture and solvent.

Ion exchange capacity (IEC) of the membranes was measured by titration. Firstly, the membrane in acid form was immersed in 50 ml 1 mol L^{-1} NaCl solution for 24 h to replace the protons of sulfonic acid groups with sodium ions, then the released protons in solution were titrated with 0.01 mol L^{-1} NaOH using phenolphthalein as the indicator.

The water uptake of the membranes was calculated by setting the weight difference between the dry and wet membranes. The dried membranes were weighed and then soaked in water. Then they were wiped with blotting paper and weighed on an analytical balance until the weight became constant. The water uptake of membranes was calculated by the following equation:

$$\text{water uptake} = \frac{W_{\text{wet}} - W_{\text{dry}}}{W_{\text{dry}}} \times 100$$

where W_{wet} and W_{dry} were the weights of the wet and dry membranes, respectively.

The swelling ratio of the membrane sample was determined by immersing it into 2 mol L^{-1} methanol aqueous solution at 80 °C for 24 h and measuring the change in length before and after the swelling. The swelling ratio was calculated by:

$$\text{swelling ratio} = \frac{L_{\text{wet}} - L_{\text{dry}}}{L_{\text{dry}}} \times 100$$

where L_{wet} and L_{dry} were the lengths of the wet and dry membrane samples, respectively.

The proton conductivity of membranes was measured using ZAHNER IM6 by two-point probe electrochemical impedance spectroscopy technique over the frequency range from 100 Hz to 3 MHz according to the method described elsewhere [13]. The membrane resistance was taken at the frequency that produced the minimum imaginary response. The conductivity of the membrane was calculated from the measured resistance, and sample dimensions with the relation $\sigma = l/R{\cdot}S$, where σ, l, R, and S are membrane conductivity, distance between two electrodes, measured resistance of membrane and cross-sectional area of the membrane perpendicular to the flow, respectively.

Methanol permeability measurement was carried out using a liquid diffusion cell composed of two compartments containing solutions A and B. The compartment A (V_A = 150 ml) was filled with 10 mol L^{-1} methanol solution. The other compartment (V_B = 150 ml) was filled with deionized water only. The membrane under test was immersed in deionized water for hydration before measurements and then vertically placed between the two compartments by a screw clamp. Both compartments were mildly stirred during the permeation experiments. Amount of methanol diffused from compartment A to B across the membrane was measured over time by a gas chromatograph (Shimadzu, GC-14B). The methanol permeability, *P* was calculated by the following equation [31]:

$$P = \frac{k \cdot V_B \cdot L}{A \cdot C_A}$$

where k was the slope of the straight-line plot of methanol concentration in solution B versus permeation time; V_B, L and A were the volume of solution B, thickness and the effective area of the membrane under test, respectively.

3. Results and discussion

3.1. Hybrid membrane preparation

Hybrid membranes were prepared using a functionalized sulfonated poly(arylene ether sulfone) and silane, according to the idealized scheme shown in Scheme 2. The thermal treatment might have resulted in the formation of crosslinking network structure linking not only polymer chains but also polymer chains with silica moieties, which caused the alteration of solubility behavior of the membranes. Pristine ANa10 membrane was readily soluble in DMAc. However, hybrid membranes lost their solubility in DMAc. Formation of a crosslinking structure in hybrid membrane should enhance the membrane stability in solvents.

Fig. 1 shows the FT-IR spectra of the membranes. The membranes exhibited typical absorption bands in spectra, including strong characteristic peaks at 1030 and 1098 cm^{-1} assigned to symmetric and asymmetric stretching of the sulfonate acid groups. Therefore, it is clear that the sulfonate acid groups were successfully introduced in the copolymers. Compared to the ANa10, new broad bands appeared at 957 cm^{-1} (characteristic of the Si–OH stretching), and at around 1200 cm^{-1} (characteristic of Si–O–Si asymmetric stretching) in the hybrid membrane, arising from the products of the sol–gel reaction. The broad absorption peak at

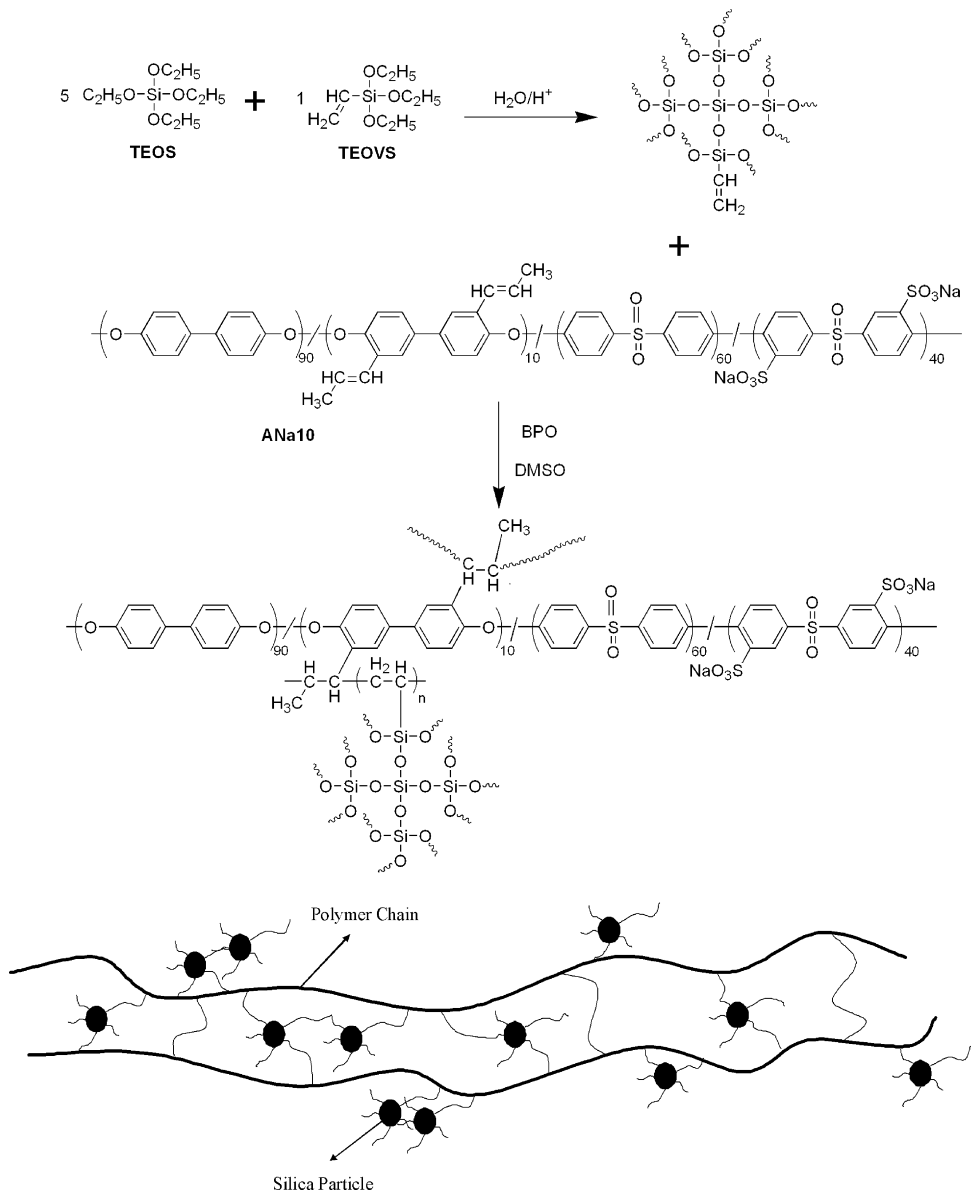

Scheme 2. Preparation and structure of crosslinked/hybrid membranes.

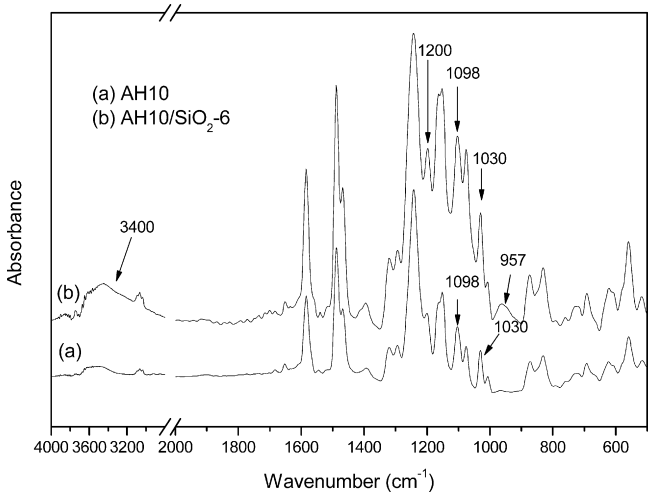

Fig. 1. FT-IR spectra of membranes.

around 3400 cm^{-1} (O–H stretching) in the hybrid membrane indicated that there were a significant number of –OH groups due to non-condensed ≡SiOH.

3.2. Morphology

ANa10/silica hybrid membranes containing 2–12 wt.% of silica were prepared. All hybrid membranes showed transparent appearance (Fig. 2) indicating the formation of very small silica nanoparticles from sol–gel process. Fig. 3 shows cross-sectional SEM images of hybrid membranes of AH10/SiO_2-6 (a) and AH10/SiO_2-12 (b). The presence of the silica particles was confirmed by EDX spectrum as shown in Fig. 4. It can be seen from Fig. 3 that the particles were on the nanoscale and no silica aggregation occurred in the hybrid membranes. The size of the silica particles in hybrid membranes slightly increased with increasing the content of silica. The average diameter of inorganic particles in AH10/SiO_2-6 membrane was no more than 30 nm. And the size of the inorganic particles in AH10/SiO_2-12 was smaller than 75 nm. The figure presented a homogeneous distribution of the silica in the

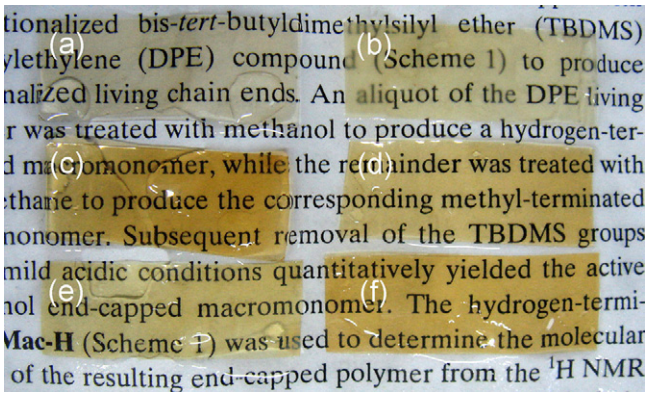

Fig. 2. Photographs of membranes: (a) AH10, (b) AH10/SiO_2-2, (c) AH10/SiO_2-6, (d) AH10/SiO_2-8, (e) AH10/SiO_2-10, and (f) AH10/SiO_2-12.

observation area indicated that the silica nanoparticles homogeneously distributed in the polymer matrix. Moreover, it was noted that the introduction of silica nanoparticles to the polymer matrix did not introduce porosity, indicating a good contact between the polymer matrix and the filler. We expect that the silica particles embedded in the membrane matrix act as a methanol barrier, and consequently methanol permeability will be reduced.

3.3. Oxidative stability

During fuel cell operation, possible degradation of the polymer electrolyte is caused by $HO^{\bullet}$ and $HO_2^{\bullet}$ radicals formed from oxygen which diffusing through the membrane and undergoing incomplete reduction [32]. Thus, the oxidative stability is one of the important factors evaluating the lifetime of PEMs under harsh fuel cell conditions. The oxidative stability to peroxide radical attack is investigated by measuring the elapsed times that a membrane began to break after immersion in Fenton's reagent (3% H_2O_2 containing 2 ppm $FeSO_4$) at 80 °C, which is one of the standard tests for oxidative stability. As shown in Fig. 5, all of the hybrid membranes showed much higher oxidative stability than the pristine AH10 membrane and the oxidative stability gradually increased with the increasing of silica content. AH10 membrane started to break after 4 h, whereas the AH10/SiO_2-12 films endured for 5.5 h before it started to dissolve. This oxidation stability was, indeed, very high for a polymer electrolyte material based on a non-fluorinated hydrocarbon skeleton. The increase in the crosslinkable silica component content led to higher degree of crosslinking and better oxidative stability. The improved oxidative stability could be attributed to the following two reasons. Firstly, crosslinkage

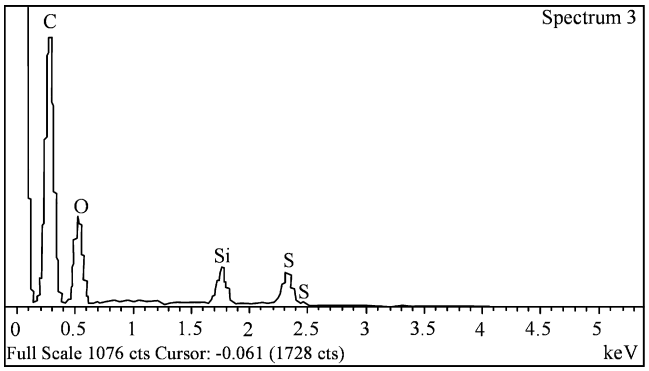

Fig. 4. EDX spectrum of AH10/SiO_2-12.

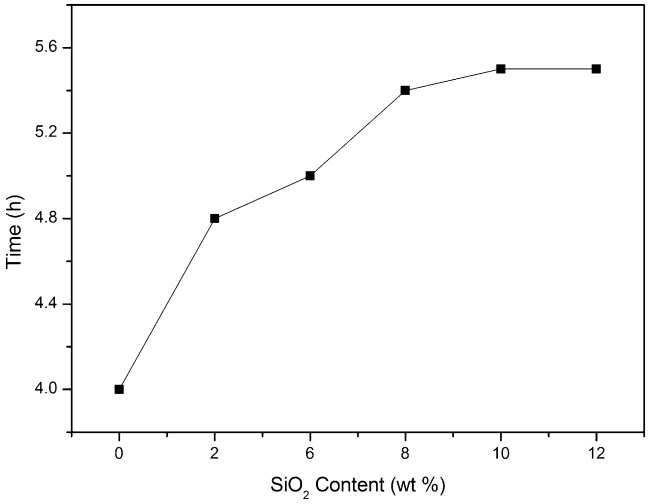

Fig. 5. Oxidative stability of AH10 and hybrid membranes at 80 °C in Fenton's reagent.

increased the packing density of polymer chains which increase the resistance of membranes opposite to radical attack. Secondly, like the reinforcement effect of crosslinkage on mechanical strength of polymer material, crosslinkage may be equal to the increase of polymer molecular weight. As a polymer chain is attacked by a radical, the broken molecular chain can be still attached on the polymer network by crosslinking point which prolong the complete broken time of polymer bone under the radical attack. Nevertheless, it is also noted that compared with Nafion, the oxidative stability

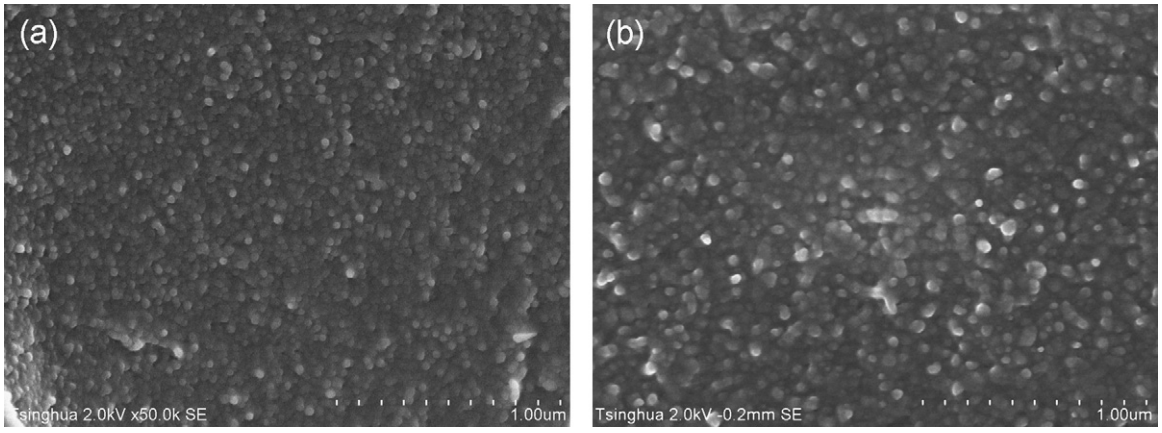

Fig. 3. Cross-sectional SEM image of membranes: (a) AH10/SiO_2-6 and (b) AH10/SiO_2-12.

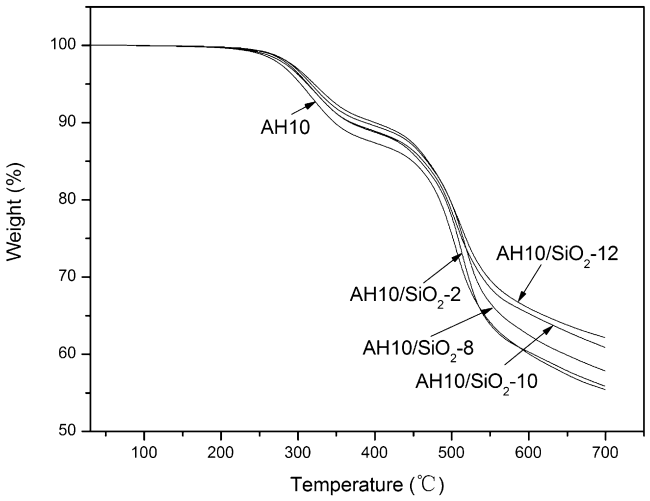

Fig. 6. TGA curves of AH10 and hybrid membranes.

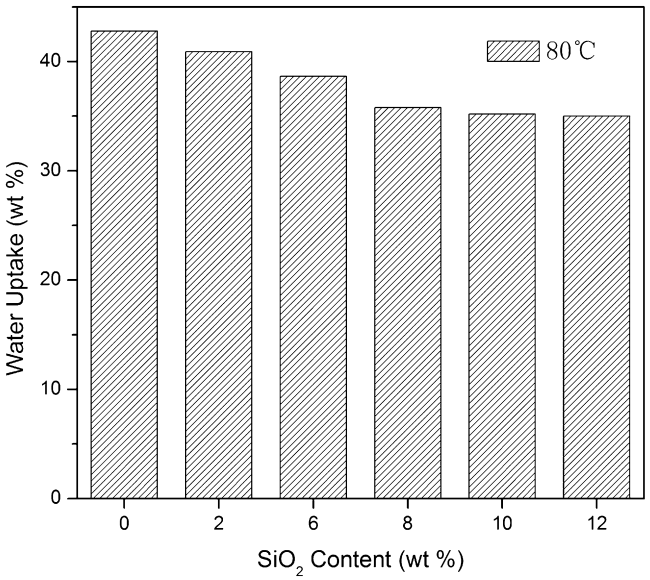

Fig. 7. Water uptake of AH10 and hybrid membranes at 80 °C.

of these membranes is still relatively poor which should greatly improved by revolutionary work.

3.4. Thermal property

The thermal stability of the AH10 and AH10/SiO_2 hybrid membranes is investigated by TGA under N_2 environment. Membrane samples for TGA analysis were preheated to 150 °C at 10 °C min^{-1} under nitrogen atmosphere and held isothermally for 30 min for moisture removal. As shown in Fig. 6, a two-step degradation profile was observed. The first weight loss region around 250–340 °C was assigned to the desulfonation. In the second weight loss region, the polymer residues were further degraded at around 360–550 °C, which corresponds to the decomposition of the polymer main chain. These two weight loss temperatures shifted toward high temperatures with increase of silica content. In the case of the hybrid membranes, the weight remaining after the polymer decomposition depended on the content of the inorganic component. That is, the weight residues of the hybrid membranes containing silica at T = 700 °C were higher than that of unfilled AH10 membrane. These results indicated that crosslinked silica frameworks in the hybrid membrane enhanced the thermal stability of the given hybrid materials.

3.5. Ion exchange capacity (IEC)

The ion exchange capacity (IEC) of the membrane plays an important role for water uptake and proton conductivity which depends on the density of hydrophilic functional groups [33]. IEC provides an indication of the ion exchangeable groups present in a membrane [34]. It can be seen in Table 1 that the IEC values of membranes decreased with the increasing of silica content, and were in the range of 1.39–1.59 m equiv. g^{-1}. Because the same polymer matrix was used here to prepare the hybrid membranes, the sulfonic acid contents were same in all the hybrid membranes. The reduction of IEC was mainly attributed to the dilution effect of the silica which was lack of the sulfonic acid group and the formation of crosslinking network. The crosslinking structure and silica component made the membrane rigid, decreased chain mobility and the swelling of the polymer network was suppressed. Therefore, the hybrid membranes had denser network structure than pristine AH10, which might result in less and smaller hydrophilic channels for proton mobility and water absorption, and hence not being available for the exchange of protons for Na^+ in the titration, the IEC values therefore decreased [20].

3.6. Water uptake and methanol swelling

In general, for ionomer membranes, the proton conductivity depends on the number of available acid groups and their dissociation capability in water, which is accompanied by the generation of protons. Water molecules dissociate acid functionality and facilitate proton transport, so the water uptake is an important parameter in studying PEMs [35]. Fig. 7 shows the water uptake of the AH10/silica hybrid membranes as a function of SiO_2 content at 80 °C. It is noted that water uptake of the hybrid membranes exhibited a decreasing tendency with an increase in SiO_2 content and leveled off for SiO_2 contents above 8 wt.%. The water uptake of the hybrid membrane with 8 wt.% SiO_2 decreased to about 84% of that of pristine AH10. It is known that crosslinking increased the interaction of the polymers and hindered chains mobility which resulted in more compact membranes with a decrease in the free volume capable of holding water molecules. An increase in the content of crosslinkable silica moieties was associated with high crosslinking density, and further restrictions on the mobility of polymer chains resulting in a decrease in the water uptake. However, sol–gel process performed at relatively low temperatures (<300 °C) might limit the gel reaction conversions resulting in silica possessing high contents of silanol groups. These retained silanol groups contribute to the highly hygroscopic character of the formed silica [36,37]. Although the free volume that could associate with the water

Table 1
Ion exchange capacity (IEC) of AH10 and hybrid membranes.

Sample	AH10	AH10/SiO_2-2	AH10/SiO_2-6	AH10/SiO_2-8	AH10/SiO_2-10	AH10/SiO_2-12
SiO_2 content (wt.%)	0	2	6	8	10	12
IEC[a] (m equiv. g^{-1})	1.59	1.54	1.48	1.45	1.42	1.39

[a] Measured IEC of the membranes by titration.

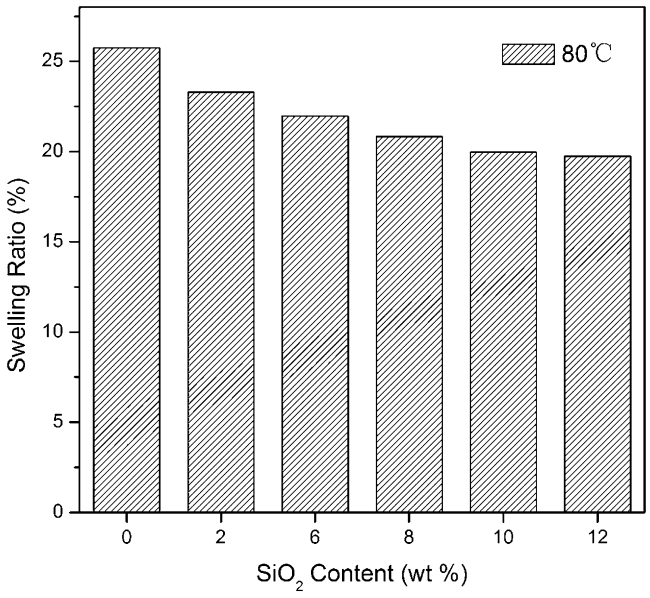

Fig. 8. Swelling ratio of AH10 and hybrid membranes at 80 °C.

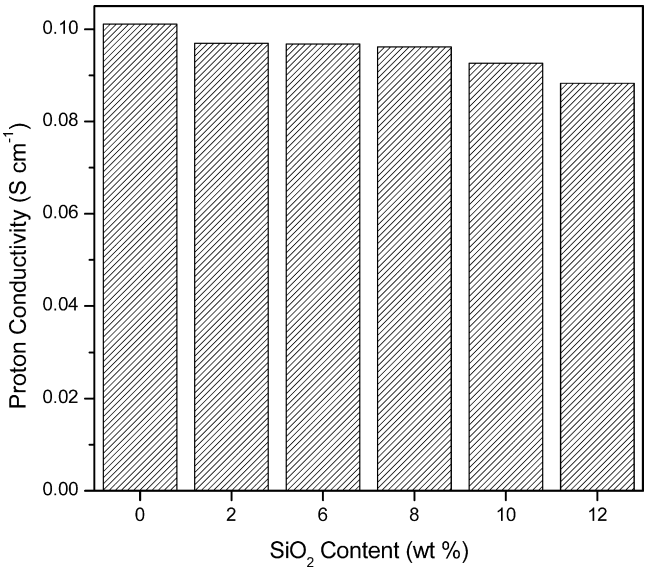

Fig. 9. Proton conductivity of AH10 and hybrid membranes at 30 °C.

molecules in the polymer structure decreased with an increasing degree of crosslinking, the silica particles could also absorb water molecules. In this study, the crosslinking effect was more prominent than the hygroscopic effect, and so the water uptake reduced slowly and leveled off with the increase in SiO_2 content.

Membrane swelling is an equally important parameter for DMFC applications. A disadvantage of most sulfonated hydrocarbon polymer membranes is extreme swelling behavior in methanol/water solution, especially at high temperature or high methanol concentration, which may cause excessive dimensional changes, uneven stresses between the membrane, electrodes and seal, resulting even in the breakage of membrane in fuel cells [19]. The swelling ratio of the AH10 and hybrid membranes in 2 mol L^{-1} methanol aqueous solution at 80 °C as a function of SiO_2 content is shown in Fig. 8. As can be seen, the swelling ratio of hybrid membranes slowly decreased from 26 to 19% with the increase of SiO_2 content from 0 to 12 wt.%. It might result from that crosslinking increased the interaction of the polymer molecules and restrained the movement of polymer chains. This might help in decreasing the methanol crossover.

3.7. Proton conductivity

In a DMFC, proton conductivity of membrane is a crucial parameter because the cell performance is strongly dependent upon this property. Higher level of proton conductivity leads to higher power density. Fig. 9 shows the proton conductivities of the AH10 and hybrid membranes at 30 °C in liquid water. As the silica content was increased, the proton conductivity of hybrid membranes decreased. It was decreased from 0.101 S cm^{-1} for pristine AH10 membrane to 0.096 S cm^{-1} for the AH10/silica hybrid membrane with 8 wt.% SiO_2 content which was only about 5% decrease compared to pristine polymer. In general, two principal mechanisms describe proton diffusion through the membranes [38,39]. One is the Grotthus mechanism (hopping mechanism) wherein a proton is passed down a chain of water molecules. The protons are transferred from one proton acceptor site to another by hydrogen bonds (proton hopping). The other is the vehicle mechanism whereby a proton combines with vehicles such as H_3O^+ or $CH_3OH_2^+$ and also with unprotonated vehicles (H_2O), thus allowing the net transport of protons. It is possible that the bound water participates by the Grotthus mechanism, and the free water takes part mostly by vehicle mechanism [40]. The decrease in proton conductivity could be resulting from the crosslinking effect of inorganic network restricting mobility of polymer chains and decreasing the free volume, which might result in less and smaller hydrophilic channels for hydrated proton transport. Further, addition of silica to AH10 might cause a reduction in density of sulfonic acid groups in the hybrid membranes so as to lower the membrane's proton conductivity. The proton conductivity of the membranes measured at various temperatures is shown in Fig. 10. The membranes exhibited high proton conductivities at elevated temperatures. The proton conductivity of A10/silica hybrid membrane with 8 wt.% SiO_2 content was 0.096 S cm^{-1} at 30 °C, but it increased to 0.241 S cm^{-1} at 80 °C. This improvement could be due to the fact that the increase in temperature promoted the molecular movement of water and activated the Grotthus proton transport process which consequently enhanced the transport of hydrated protons.

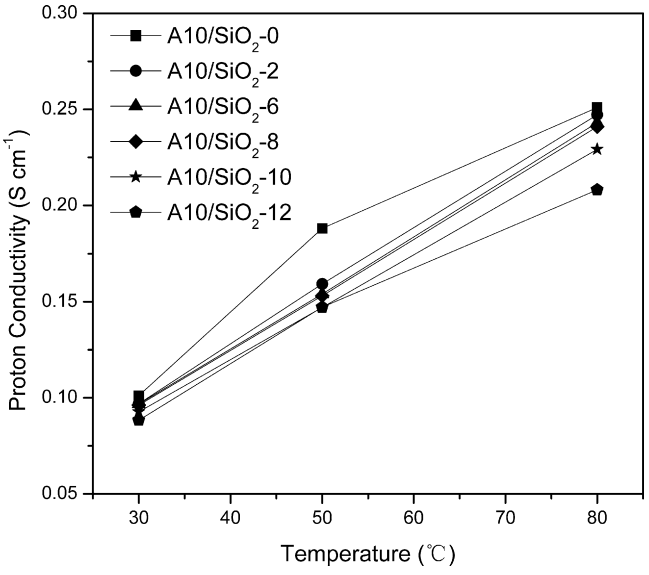

Fig. 10. Proton conductivity of AH10 and hybrid membranes at different temperatures.

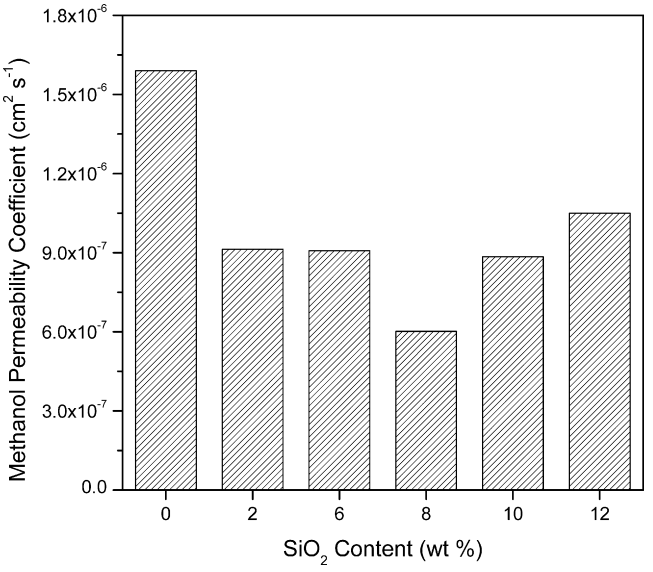

Fig. 11. Methanol permeability coefficient of AH10 and hybrid membranes at 30 °C.

3.8. Methanol permeability

To evaluate the practicality of using hybrid membranes in DMFCs, methanol permeability coefficient was measured and is shown in Fig. 11. It is noted that the methanol permeability coefficient of the hybrid membranes decreased at first and then increased. With silica content up to about 8 wt.%, the methanol permeability coefficients had the minimum of 6.02×10^{-7} cm^2 s^{-1}, a 2.64-fold decrease compared to that of the pristine membrane. The reduction in methanol permeability coefficient might result from the silica particles in the polymer matrix acting as methanol barriers, which inhibit the methanol crossover through the membranes. In addition, crosslinking could effectively hinder the polymer chain mobility and suppress the swelling of network in aqueous methanol solution, which reduced the number of channels to pass methanol molecules and therefore increasing the resistance to methanol diffusion. Increased silica content resulted in more block and crosslinking density, decreasing the methanol crossover of the membranes. However, over a silica content of 8 wt.%, the methanol permeability coefficient of the hybrid membranes increased gradually. This might be result from the average diameter of silica nanoparticles gradually increased with the increasing the content of silica. The bigger silica particles in hybrid membranes decreased the resistance opportunity for methanol transport, which resulted in more methanol crossover through membranes. Hence, small silica particle size and highly crosslinking degree are preferred for hybrid membranes with excellent methanol barrier property.

4. Conclusions

Sulfonated poly(arylene ether sulfone) (SPAES) pendant propenyl moiety was synthesized from 4,4′-biphenol (BP), 3,3′-diallyl-4,4′-dihydroxybiphenyl (ABP), 4,4′-dichloro diphenylsulfone (DCDPS) and 3,3′-disulfonated-4,4′-dichlorodiphenyl sulfone (SDCDPS). From SPAES, a series of hybrid membranes incorporating different amounts of silica nanoparticles were prepared using the sol–gel reaction with triethoxyvinylsilane (TEOVS) and tetraethoxysilane (TEOS). The hybrid membranes were then thermally crosslinked in the presence of benzoyl peroxide (BPO) initiator for formation the crosslinked structure and the covalent bonding between the polymer chains and silica moieties. The introduction of the covalent bonding between polymer chains and silica nanoparticles resulted in reinforcing interfacial interaction between two phases. The study showed that the crosslinking and introduction of silica led to the reduction of methanol swelling and water uptake. Moreover, the oxidative stability and thermal stability of the hybrid membranes were improved. The methanol permeability coefficient decreased with silica content up to about 8 wt.%, and above this concentration, the property increased with silica content. Although the proton conductivity slightly decreased, the overall performance of the hybrid membranes was considerably improved by crosslinking and the addition of silica.

Acknowledgements

The work is funded by the National Natural Science Foundation of China (50703021 and 50911140287) and National High Technology R&D Program of China (2007AA05Z146, 2007AA05Z150 and 2008AA03Z205).

References

[1] X.M. Ren, M.S. Wilson, S. Gottesfeld, J. Electrochem. Soc. 143 (1996) L12–L15.
[2] A.S. Arico, P. Creti, P.L. Antonucci, J. Cho, H. Kim, V. Antonucci, Electrochim. Acta 43 (1998) 3719–3729.
[3] S.P. Jiang, Z.C. Liu, Z.Q. Tian, Adv. Mater. 18 (2006) 1068–1072.
[4] A. Heinzel, V.M. Barragan, J. Power Sources 84 (1999) 70–74.
[5] K. Scott, W.M. Taama, P. Argyropoulos, J. Power Sources 79 (1999) 43–59.
[6] A. Siu, B. Pivovar, J. Horsfall, K.V. Lovell, S. Holdcroft, J. Polym. Sci. Part B: Polym. Phys. 44 (2006) 2240–2252.
[7] D.H. Jung, Y.B. Myoung, S.Y. Cho, D.R. Shin, D.H. Peck, Int. J. Hydrog. Energy 26 (2001) 1263–1269.
[8] E. Chalkova, M.V. Fedkin, S. Komarneni, S.N. Lvov, J. Electrochem. Soc. 154 (2007) B288–B295.
[9] D.S. Kim, B. Liu, M.D. Guiver, Polymer 47 (2006) 7871–7880.
[10] R.H. He, Q.F. Li, A. Bach, J.O. Jensen, N.J. Bjerrum, J. Membr. Sci. 277 (2006) 38–45.
[11] D.J. Jones, J. Roziere, J. Membr. Sci. 185 (2001) 41–58.
[12] R.H. He, Q.F. Li, G. Xiao, N.J. Bjerrum, J. Membr. Sci. 226 (2003) 169–184.
[13] F. Wang, M. Hickner, Y.S. Kim, T.A. Zawodzinski, J.E. McGrath, J. Membr. Sci. 197 (2002) 231–242.
[14] Y.X. Li, F. Wang, J. Yang, D. Liu, A. Roy, S. Case, J. Lesko, J.E. McGrath, Polymer 47 (2006) 4210–4217.
[15] W.L. Harrison, F. Wang, J.B. Mecham, V.A. Bhanu, M. Hill, Y.S. Kim, J.E. McGrath, J. Polym. Sci. Part A: Polym. Chem. 41 (2003) 2264–2276.
[16] K.D. Kreuer, J. Membr. Sci. 185 (2001) 29–39.
[17] C.H. Lee, H.B. Park, Y.S. Chung, Y.M. Lee, B.D. Freeman, Macromolecules 39 (2006) 755–764.
[18] P.C. Deb, L.D. Rajput, V.R. Hande, S. Sasane, A. Kumar, Polym. Adv. Technol. 18 (2007) 419–426.
[19] F.C. Ding, S.J. Wang, M. Xiao, Y.Z. Meng, J. Power Sources 164 (2007) 488–495.
[20] S. Zhong, X. Cui, H. Cai, T. Fu, C. Zhao, H. Na, J. Power Sources 164 (2007) 65–72.
[21] S. Feng, Y. Shang, X. Xie, Y. Wang, J. Xu, J. Membr. Sci. 335 (2009) 13–20.
[22] J. Chen, Y. Maekawa, M. Asano, M. Yoshida, Polymer 48 (2007) 6002–6009.
[23] I. Homna, H. Nakajima, S. Nomura, Solid State Ionics 154 (2002) 707–712.
[24] B. Ruffmann, H. Silva, B. Schulte, S.P. Nunes, Solid State Ionics 162 (2003) 269–275.
[25] I. Honma, H. Nakajima, O. Nishikawa, T. Sugimoto, S. Nomura, Solid State Ionics 162 (2003) 237–245.
[26] R.Q. Fu, J.J. Woo, S.J. Seo, J.S. Lee, S.H. Moon, J. Power Sources 179 (2008) 458–466.
[27] S.W. Chuang, S.L.C. Hsu, Y.H. Liu, J. Membr. Sci. 305 (2007) 353–363.
[28] H.Y. Chang, C.W. Lin, J. Membr. Sci. 218 (2003) 295–306.
[29] U. Caruso, P. Iannelli, A. Roviello, A. Sirigu, J. Polym. Sci. Part B: Polym. Phys. 36 (1998) 2371–2378.
[30] M. Sankir, V.A. Bhanu, W.L. Harrison, H. Ghassemi, K.B. Wiles, T.E. Glass, A.E. Brink, M.H. Brink, J.E. McGrath, J. Appl. Polym. Sci. 100 (2006) 4595–4602.
[31] Y. Woo, S.Y. Oh, Y.S. Kang, B. Jung, J. Membr. Sci. 220 (2003) 31–45.
[32] G. Hubner, E. Roduner, J. Mater. Chem. 9 (1999) 409–418.
[33] H.C. Lee, H.S. Hong, Y.-M. Kim, S.H. Choi, M.Z. Hong, H.S. Lee, K. Kim, Electrochim. Acta 49 (2004) 2315–2323.
[34] B. Smitha, S. Sridhar, A.A. Khan, Macromolecules 37 (2004) 2233–2239.
[35] P.X. Xing, G.P. Robertson, M.D. Guiver, S.D. Mikhailenko, K.P. Wang, S. Kaliaguine, J. Membr. Sci. 229 (2004) 95–106.
[36] Y.H. Su, Y.L. Liu, Y.M. Sun, J.Y. Lai, M.D. Guiver, Y. Gao, J. Power Sources 155 (2006) 111–117.
[37] N. Miyake, J.S. Wainright, R.F. Savinell, J. Electrochem. Soc. 148 (2001) A898–A904.
[38] K.D. Kreuer, Chem. Mater. 8 (1996) 610–641.
[39] D.S. Kim, H.B. Park, J.W. Rhim, Y.M. Lee, Solid State Ionics 176 (2005) 117–126.
[40] Y.H. Su, Y.L. Liu, Y.M. Sun, J.Y. Lai, D.M. Wang, Y. Gao, B.J. Liu, M.D. Guiver, J. Membr. Sci. 296 (2007) 21–28.